Improved Semipolar (11$\bar{2}$2) GaN Quality Grown on *m*-Plane Sapphire Substrates by Metal Organic Chemical Vapor Deposition Using Self-Organized SiN_x Interlayer *

Sheng-Rui Xu(许晟瑞)[1], Ying Zhao(赵颖)[1], Teng Jiang(姜腾)[1], Jin-Cheng Zhang(张进成)[1**], Pei-Xian Li(李培咸)[2**], Yue Hao(郝跃)[1]

[1]*Key Laboratory of Wide Band-Gap Semiconductor Technology, School of Microelectronics, Xidian University, Xi'an 710071*

[2]*School of Advanced Materials and Nanotechnology, Xidian University, Xi'an 710071*

(Received 29 January 2016)

The effect of a self-organized SiN_x interlayer on the defect density of (11$\bar{2}$2) semipolar GaN grown on m-plane sapphire is studied by transmission electron microscopy, atomic force microscopy and high resolution x-ray diffraction. The SiN_x interlayer reduces the c-type dislocation density from $2.5 \times 10^{10}\,cm^{-2}$ to $5 \times 10^{8}\,cm^{-2}$. The SiN_x interlayer produces regions that are free from basal plane stacking faults (BSFs) and dislocations. The overall BSF density is reduced from $2.1 \times 10^{5}\,cm^{-1}$ to $1.3 \times 10^{4}\,cm^{-1}$. The large dislocations and BSF reduction in semipolar (11$\bar{2}$2) GaN with the SiN_x interlayer result from two primary mechanisms. The first mechanism is the direct dislocation blocking by the SiN_x interlayer, and the second mechanism is associated with the unique structure character of (11$\bar{2}$2) semipolar GaN.

PACS: 81.15.Gh, 81.10.Aj, 71.55.Eq, 78.55.Ap DOI: 10.1088/0256-307X/33/6/068102

It is well known that the hexagonal GaN-based film and its alloys grown along the polar (0001) *c*-axis exhibit strong spontaneous polarization and strain-induced polarization which reduce the radiative recombination efficiency and redshift the emission wavelength of devices grown in this orientation, and this phenomenon is called the quantum-confined Stark effect (QCSE). The problem of the QCSE can be avoided by growing the GaN film in the 'nonpolar' orientations (the *a* or *m* orientation).[1,2] The electric field can also be reduced by growing in the so-called 'semipolar' orientation, among all semipolar planes, the semipolar (11$\bar{2}$2) plane was reported to have binding sites that may accommodate indium atoms more easily than either the *c*-plane or the *m*-plane.[3,4] Furthermore, numerous long wavelength high efficiency green light emitting diodes (LEDs), yellow LEDs, and amber LEDs have been demonstrated on this plane bulk substrate.[5–7] However, the very small size and high cost of the bulk substrate is not suitable for large-scale industrial applications. Fortunately, semipolar (11$\bar{2}$2) GaN can be obtained by metalorganic chemical vapor deposition (MOCVD) on the *m*-plane (1$\bar{1}$00) sapphire.[8–10] However, it has been reported that heteroepitaxially semipolar (11$\bar{2}$2) GaN films grown on the *m*-plane sapphire substrate exhibit poor crystal quality with very high threading dislocations (TDs) of $\sim 10^{10}\,cm^{-2}$ and high basal stacking faults (BSFs) of $\sim 10^{5}\,cm^{-1}$,[2,9,10] which could act as non-radiative recombination centers and could reduce the quantum efficiency in LEDs. Traditional epitaxial lateral overgrowth (ELOG) is a widely used defect reduction technique that needs the complex lithography process,[11–13] and this technique has been used for the growth of semipolar (11$\bar{2}$2) GaN.[10,14] Thus the growth method without a mask patterning step was therefore highly desirable at this time.

In this Letter, the effect of the self-organized SiN_x interlayer on the microstructure and defect density of the (11$\bar{2}$2) semipolar GaN thin film grown on (1$\bar{1}$00) *m*-plane sapphire is investigated by transmission electron microscopy (TEM) atomic force microscopy (AFM), and high resolution x-ray diffraction (HRXRD).

For sample A, firstly, *m*-sapphire was nitrided during temperature ramping up to 1020℃ in an ammonia environment to suppress the formation of mixed phase semipolar (10$\bar{1}$3) grains, then a 20-nm-thick GaN low-temperature nucleation layer was grown on the *m*-sapphire at 560℃. Secondly, a 1.6-μm-thick semipolar (11$\bar{2}$2) GaN template was grown on the low-temperature nucleation layer at 1000℃ and 40 Torr. Then the SiN_x interlayer was deposited by the plasma enhanced chemical vapor deposition (oerlikon 790) with only 5 s. The deposition of SiN_x was performed at 300℃ by using SiH_4, He and N_2 gases with the rf power of 300 W, respectively. Finally, a 6.5-μm-thick GaN layer was grown at 1040℃ and 40 Torr, hydrogen was used as the carrier gas, and triethylgallium, trimethylindium, and ammonia were used as the sources of Ga, In, and N, respectively. The semipolar (11$\bar{2}$2) GaN without the SiN_x interlayer was also grown as a control sample (sample B).

The $2 \times 2\,\mu m^2$ AFM images with contact mode of

*Supported by the National Natural Science Foundation of China under Grant Nos 61204006 and 61574108, the Fundamental Research Funds for the Central Universities under Grant No JB141101, and the Foundation of Key Laboratory of Nanodevices and Applications of Suzhou Institute of Nano-Tech and Nano-Bionics of Chinese Academy of Sciences under Grant No 15CS01.

**Corresponding author. Email: jchzhang@xidian.edu.cn; pxli@mail.xidian.edu.cn

© 2016 Chinese Physical Society and IOP Publishing Ltd

the two semipolar (11$\bar{2}$2) GaN samples are shown in Fig. 1. For sample B, similar to the results of previous nonpolar and semipolar GaN, slate-like patterns are clearly observed on the film surface.[14,15] It is well known that these slate features not only prove strong morphological anisotropy, but also could reflect density of BSFs.[16] The AFM result clearly revealed that sample B has a much higher density of the striations than sample A, which indicates that sample A has a lower density of BSFs than sample B. The rms roughnesses of samples A and B are 5.88 nm and 12.55 nm, respectively.

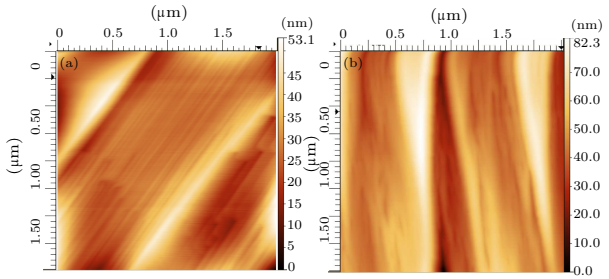

Fig. 1. The 2×2 μm^2 AFM images for samples A (a) and B (b).

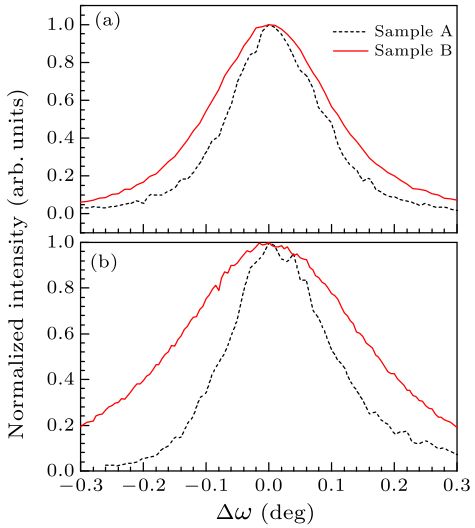

Fig. 2. Symmetric (11$\bar{2}$2) (a) and asymmetric (11$\bar{1}$1) (b) reflection HRXRD ω-scan XRC result.

For the purpose of revealing the characteristics and density of the planar and line defects, and to obtain system information of the microstructure of the as-grown semipolar (11$\bar{2}$2) GaN and its correlation with the growth dynamics, we measured x-ray rocking curves (XRCs) for both on-axis and off-axis diffraction planes by HRXRD. The HRXRD was performed by using the Bruker D8-discover system equipped with a Ge(220) monochromator and a channel-cut analyzer operating in the triple-axis mode, delivering a pure CuKα line of wavelength $\lambda = 0.15406$ nm. The normalized full width at half maximum (FWHM) of the on-axis (11$\bar{2}$2) GaN XRCs when the x-ray rocking direction was parallel to [$\bar{1}\bar{1}$23] (the surface striation direction) is shown in Fig. 2(a). As can be seen, the FWHM of the XRC was 0.16° for sample A, which was much smaller than the FWHM value 0.22° of sample B. The skew symmetric geometry for the off-axis (11$\bar{1}$1) plane which has an inclination angle $\chi = 26°$ with respect to (11$\bar{2}$2) was also used to evaluate the mosaic twist of (11$\bar{2}$2) GaN. Figure 2(b) shows that compared with sample B without the SiN_x interlayer, the FWHM of sample A was narrowed down by nearly 50%, which evidences that the self-organized SiN_x technique could significantly improve the crystal quality of (11$\bar{2}$2) GaN.

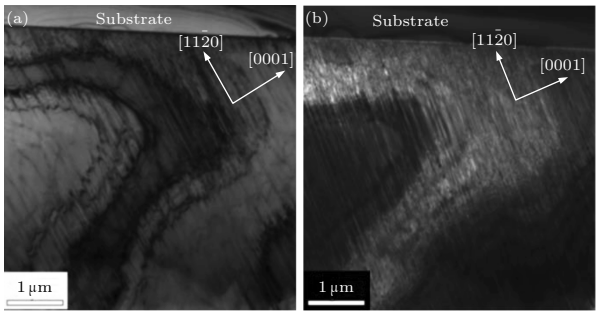

Fig. 3. Cross-sectional TEM images of sample B: (a) using g=0002 so that dislocations with a c-component are in contrast, and (b) using g=10$\bar{1}$0 thus BSFs are edge-on and in contrast.

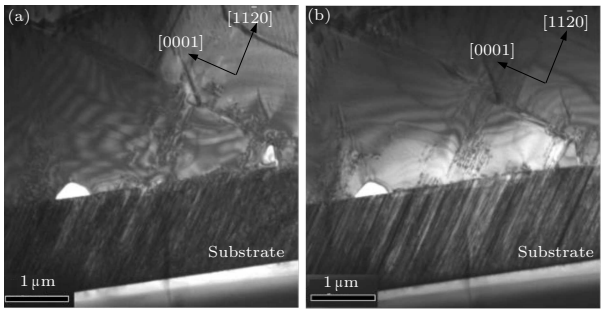

Fig. 4. Cross-sectional TEM images of sample A: (a) using g=0002 so that dislocations with a c-component are in contrast, and (b) using g=10$\bar{1}$0 thus BSFs are edge-on and in contrast.

TEM samples were prepared by mechanical polishing before ion beam thinning to electron transparency. TEM images were acquired on a Tecnai G2 F20 S-Twin operating at 200 kV. Figure 3(a) shows the cross-sectional TEM image of the sample B viewed along [1$\bar{1}$00] using g = 0002, thus the dislocations with c-component are in contrast. Figure 3(b) shows the cross-sectional TEM image of sample B by using g=1$\bar{1}$00, thus the BSFs are in contrast.[2] It can be found that the semipolar (11$\bar{2}$2) GaN without the SiN_x interlayer has a very high density of dislocations ($\sim 2.5 \times 10^{10}$ cm^{-2}) and BSFs ($\sim 2.1 \times 10^{5}$ cm^{-1}). The dislocation in the layer is nearly the same from the substrate to the surface, and this indicates that the dislocations and BSFs cannot be reduced by only increasing the thickness of GaN.

Figure 4(a) is viewed along [1$\bar{1}$00] by using g=0002

of sample A, thus the dislocations with c-component are in contrast. The dislocation density is very low in the overgrown layer after the filter of the SiN_x interlayer and large dislocation free regions are visible. BSFs are in contrast in Fig. 4(b) by using g=10$\bar{1}$0. It is obvious that the dislocations and BSFs are significantly reduced. The c-type dislocation density is reduced over two orders of magnitude to $5\times10^8\,\mathrm{cm}^{-2}$, the average BSF density is reduced by a factor of 16 to $1.3\times10^4\,\mathrm{cm}^{-1}$. Large defect free regions over the SiN_x interlayer are obtained. Furthermore, after the blocking effect of the SiN_x, the density of dislocations and the BSFs were further decreased. In fact, if there is no other dislocation blocking mechanism, the dislocation density of the overgrowth GaN layer may directly terminate by the covered proportion of SiN_x.

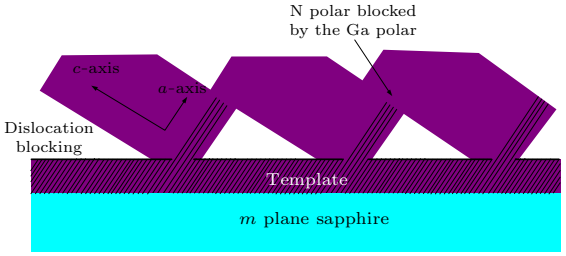

Fig. 5. Schematic image of the dislocations reduction mechanism during over growth of sample A.

We attribute the large dislocations and BSF reduction in the semipolar (11$\bar{2}$2) GaN resulting from the SiN_x interlayer to two primary mechanisms. The first mechanism is the direct dislocation blocking by the SiN_x interlayer, which is revealed in the cross-sectional TEM images as shown in Fig. 4. The additional mechanism for dislocations and BSF reduction is associated with the unique structure character of (11$\bar{2}$2) semipolar GaN. The defects originating in the template layer run through the film at an angle of 58° with the substrate in the region where there is no SiN_x mask. Generally, the growth along the $+c$-axis is faster than that in the $-c$-direction,[17] thus when the crystal grain expands over the SiN_x mask, it grows preferentially along the $+c$-direction. The coalescence occurs when the $+c$- and $-c$-facets (Ga polar and N polar) meet. In this situation, the dislocations and BSFs propagating along the a-axis were blocked by the nearby Ga polar wing, and were free to propagate from the window toward the surface as shown schematically in Fig. 5. The significant difference of dislocations reduction mechanism in semipolar GaN and nonpolar GaN is that the nonpolar GaN only terminated by the cover rate of SiN_x or SiO_2, while the semipolar GaN has a second annihilation process.[18,19]

In summary, a simple technique for growing high quality (11$\bar{2}$2) GaN on 2 in sapphire with very low TDs and BSFs by using the self-organized SiN_x interlayer as a dislocation filtering dielectric growth mask has been demonstrated. Compared with the conventional epitaxial lateral overgrowth method, this technique does not require expensive lithographic patterning steps or equipment. Due to the inclined direction of the c-axis, the crystal can expand above the adjacent crystal, thus stopping the propagation of TDs and BSFs. In this case, defect-free regions were present in the overgrown layer.

We thank Niu Mutong (Suzhou Institute of Nano-Tech and Nano-Bionics) for performing the TEM and Optoelectronics measurements of GaN.

References

[1] Waltereit P, Brandt O, Trampert A, Grahn H T, Menniger J, Ramsteiner M, Reiche M and Ploog K H 2000 *Nature* **406** 865
[2] Johnston C F, Moram M A, Kappers M J and Humphreys C J 2009 *Appl. Phys. Lett.* **94** 161109
[3] Xu S R, Hao Y, Zhang J C, Jiang T, Yang L, Lu X and Lin Z Y 2013 *Nano Lett.* **13** 3654
[4] Xu S R, Lin Z Y, Xue X Y, Liu Z Y, Ma J C, Jiang T, Mao W, Wang D H, Zhang J C and Hao Y 2012 *Chin. Phys. Lett.* **29** 017803
[5] Sato H, Tyagi A, Zhong H, Fellows N, Chung R B, Saito M, Fujito K, Speck, J S, DenBaars S P and Nakamura S 2007 *Phys. Status Solidi* **1** 162
[6] Sato H, Chung R B, Hirasawa H, Fellows N, Masui H, Wu F, Saito M, Fujito K, Speck J S and DenBaars S P 2008 *Appl. Phys. Lett.* **92** 221110
[7] Funato M, Ueda M and Kawakami Y 2006 *Jpn. J. Appl. Phys.* **45** L659
[8] Sun Q, Leung B, Yerino C D, Zhang Y and Han J 2009 *Appl. Phys. Lett.* **95** 231904
[9] Kappers M J, Hollander J, McAleese C, Johnston C F, Broom, R F, Barnard J S, Vickers M E and Humphreys C J 2007 *J. Cryst. Growth* **300** 155
[10] Mierry P D, Kriouche N, Nemoz M and Nataf G 2009 *Appl. Phys. Lett.* **94** 191903
[11] Sakai A, Sunakawa H and Akira U 1997 *Appl. Phys. Lett.* **71** 2259
[12] Park J, Grudowski P A, Eiting C J and Dupuis R D 1998 *Appl. Phys. Lett.* **73** 333
[13] Wuu D S, Wang W K, Wen K S, Huang S C, Lin S H, Huang S Y, Lin C F and Horng R H 2006 *Appl. Phys. Lett.* **89** 161105
[14] Armitage R and Hirayama H 2008 *Appl. Phys. Lett.* **92** 092121
[15] Wei T B, Hu Q, Duan R F, Wei X C, Huo Z Q, Wang J X, Zeng Y P, Wang G H and Li J M 2009 *J. Cryst. Growth* **311** 4153
[16] Ni X, Özgür Ü Baski A A, Morkoc H, Zhou L, Smith D J and Tran C A 2007 *Appl. Phys. Lett.* **90** 182109
[17] Imer B, Wu F, Speck J S and DenBaars S P 2007 *J. Cryst. Growth* **306** 330
[18] Jiang T, Xu S R, Zhang J C, Xie Y and Hao Y 2016 *Sci. Rep.* **6** 19955
[19] Zhou X W, Xu S R, Zhang J C, Dang J Y, Lv L, Hao Y and Guo L X 2012 *Chin. Phys.* B **21** 067803